

REPORT 1144

AERODYNAMIC CHARACTERISTICS OF A REFINED DEEP-STEP PLANING-TAIL FLYING-BOAT HULL WITH VARIOUS FOREBODY AND AFTERBODY SHAPES¹

By JOHN M. RIEBE and RODGER L. NAESETH

SUMMARY

An investigation was made in the Langley 300 MPH 7- by 10-foot tunnel to determine the aerodynamic characteristics of a refined deep-step planing-tail hull with various forebody and afterbody shapes. For comparison, tests were made on a streamline body simulating the fuselage of a modern transport airplane.

The results of the tests, which include the interference effects of a 21-percent-thick support wing, indicated that for corresponding configurations the hull models incorporating a forebody with a length-beam ratio of 7 had lower minimum drag coefficients than the hull models incorporating a forebody with a length-beam ratio of 5. The lowest minimum drag coefficients, 0.0024 and 0.0023, which were considerably less than that of a comparable conventional hull of length-beam ratio 9, were obtained on the length-beam-ratio-7 forebody, alone and with round center boom, respectively. The streamline body had a minimum drag coefficient of 0.0025; flying-boat hulls can, therefore, have drag values comparable to landplane fuselages. The hull angle of attack for minimum drag varied from 2° to 4°.

Longitudinal and lateral stability was generally about the same for all hull models tested and about the same as that of a conventional hull.

INTRODUCTION

Because of the requirements for increased range and speed in flying boats, an investigation of the aerodynamic characteristics of flying-boat hulls as affected by hull dimensions and hull shape is being conducted at the Langley Aeronautical Laboratory. The results of one phase of this investigation, presented in reference 1, have indicated that hull drag can be reduced without causing large changes in aerodynamic stability and hydrodynamic performance by the use of high length-beam ratios. Another phase of the investigation, reference 2, indicated that hulls of the deep-step planing-tail type have much lower air drag than the conventional type of hull and about the same aerodynamic stability; tank tests, reference 3, have indicated that this type of hull also has hydrodynamic performance equal to and in some respects superior to the conventional type of hull.

In an attempt to improve the aerodynamic performance of hulls still further without causing excessive penalties in hydrodynamic performance, several refined deep-step planing-tail hulls were designed jointly by the Hydrodynamics

Division and the Stability Research Division of the Langley Laboratory. It was believed that improved aerodynamic performance could be facilitated mainly by refinement of the forebody plan form and by a reduction in the volume and surface area of the afterbody. This report presents the results of the tests of these hulls.

In order to make a preliminary study of overall flying-boat configurations, tests were also made on models incorporating a typical engine nacelle and an engine nacelle extended into a boom which is to function as the afterbody and reduce the size of and possibly eliminate wing-tip floats; the nacelle and nacelle boom were also tested without the hull models. For comparing the drag and stability, tests were made on a streamline body simulating the fuselage of a modern transport airplane.

Tank tests (ref. 4) have indicated that the hull models presented in the present report (with the possible exception of the forebody alone for which data are not available) will have acceptable hydrodynamic performance.

COEFFICIENTS AND SYMBOLS

The results of the tests are presented as standard NACA coefficients of forces and moments. Rolling-, yawing-, and pitching-moment coefficients are given about the locations (wing 30-percent-chord point) shown in figures 1, 2, and 3. The wing area, mean aerodynamic chord, and span used in determining the coefficients and Reynolds numbers are those of a hypothetical flying boat (ref. 1). The hull, fuselage, and nacelle coefficients were derived by subtraction of data for the wing alone from data for the wing plus hull, fuselage, or nacelle. The wing-alone data were determined by including in the tests that part of the wing which is enclosed in the hull, fuselage, or nacelle. The hull, fuselage, and nacelle coefficients therefore include the wing interference resulting from the interaction of the velocity fields of the wing and the bodies and also the negative wing interference caused by shielding from the airstream that part of the wing enclosed within the hull, fuselage, or nacelle. The data are referred to the stability axes, which are a system of axes having their origin at the center of moments shown in figures 1, 2, and 3 and in which the Z-axis is in the plane of symmetry and perpendicular to the relative wind, the X-axis is in the plane of symmetry and perpendicular to the Z-axis, and the Y-axis

¹ Supersedes NACA TN 2489, "Aerodynamic Characteristics of a Refined Deep-Step Planing-Tail Flying-Boat Hull With Various Forebody and Afterbody Shapes" by John M. Riebe and Rodger L. Naeseth, 1952.

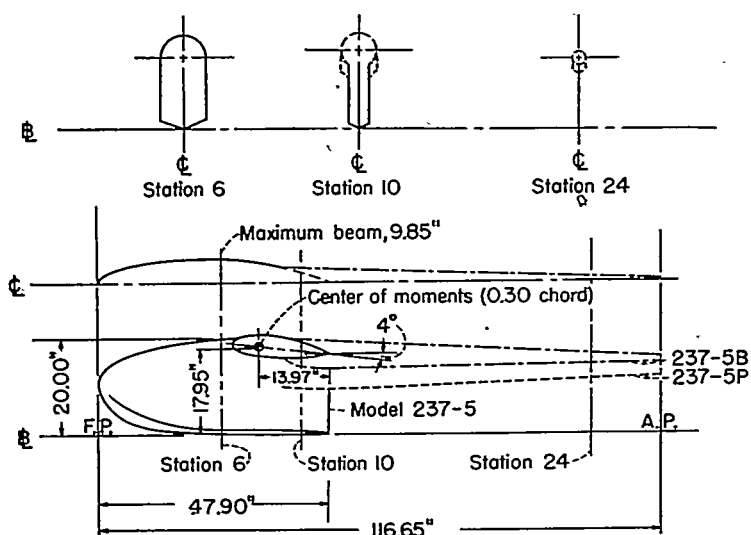


FIGURE 1.—Lines of Langley tank models 237-5, 237-5B, and 237-5P.

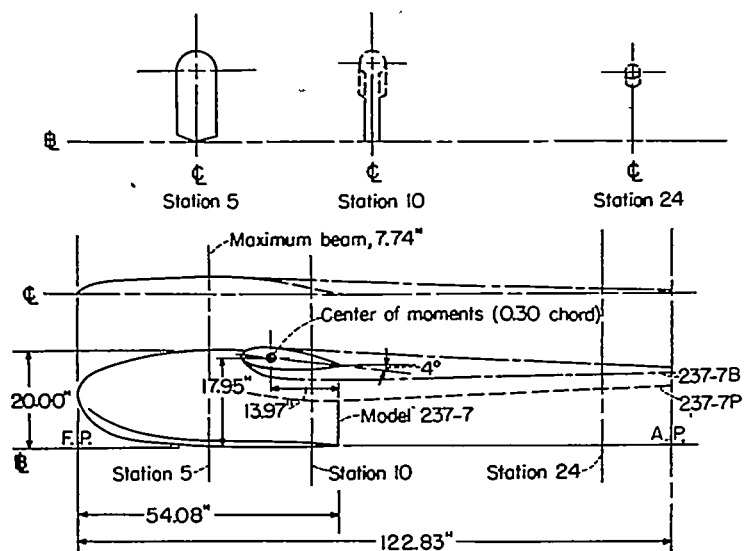


FIGURE 2.—Lines of Langley tank models 237-7, 237-7B, and 237-7P.

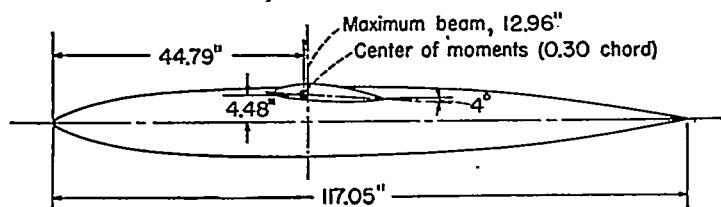
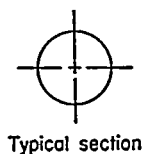


FIGURE 3.—Lines of the streamline fuselage.

is perpendicular to the plane of symmetry. The positive directions of forces and moments about the stability axes are shown in figure 4.

The coefficients and symbols are defined as follows:

C_L	lift coefficient, $Lift/qS$ where $Lift = -Z$
C_D	drag coefficient, D/qS
C_Y	lateral-force coefficient, Y/qS
C_l	rolling-moment coefficient, L/qSb
C_m	pitching-moment coefficient, $M/qS\bar{c}$
C_n	yawing-moment coefficient, N/qSb
D	drag, $-X$ when $\beta = 0$
X	force along X -axis, lb
Y	force along Y -axis, lb
Z	force along Z -axis, lb
L	rolling moment, ft-lb
M	pitching moment, ft-lb
N	yawing moment, ft-lb
q	free-stream dynamic pressure, $\rho V^2/2$, lb/sq ft
S	wing area of $\frac{1}{10}$ -scale model of hypothetical flying boat, 18.264 sq ft
\bar{c}	wing mean aerodynamic chord of $\frac{1}{10}$ -scale model of hypothetical flying boat, 1.377 ft
b	wing span of $\frac{1}{10}$ -scale model of hypothetical flying boat, 13.971 ft
V	air velocity, fps
ρ	mass density of air, slugs/cu ft
α	angle of attack of hull base line, deg
β	angle of sideslip, deg
R	Reynolds number, based on wing mean aerodynamic chord of $\frac{1}{10}$ -scale model of hypothetical flying boat

$$C_{m_\alpha} = \frac{\partial C_m}{\partial \alpha}$$

$$C_{n_\beta} = \frac{\partial C_n}{\partial \beta}$$

$$C_{Y_\beta} = \frac{\partial C_Y}{\partial \beta}$$

MODELS AND APPARATUS

The hull lines were determined through the joint cooperation of the Hydrodynamics Division and the Stability Research Division of the Langley Laboratory. The hull forebodies were derived in plan form from modified NACA 16-series symmetrical airfoil sections of thickness ratios 20 and 14.3 percent airfoil chord, resulting in forebody length-beam ratios of approximately 5 and 7, respectively. The forebody length-beam ratio is equal to the distance from the forward perpendicular (F. P.) to the step divided by the maximum beam of the forebody (figs. 1 and 2 show maximum beam of forebody). Dimensions of the hulls are given in figures 1 and 2 and tables I to IV. The lines of a tail float used for several of the tests are given in figure 5; offsets are given in table V. The streamline body, fineness ratio of

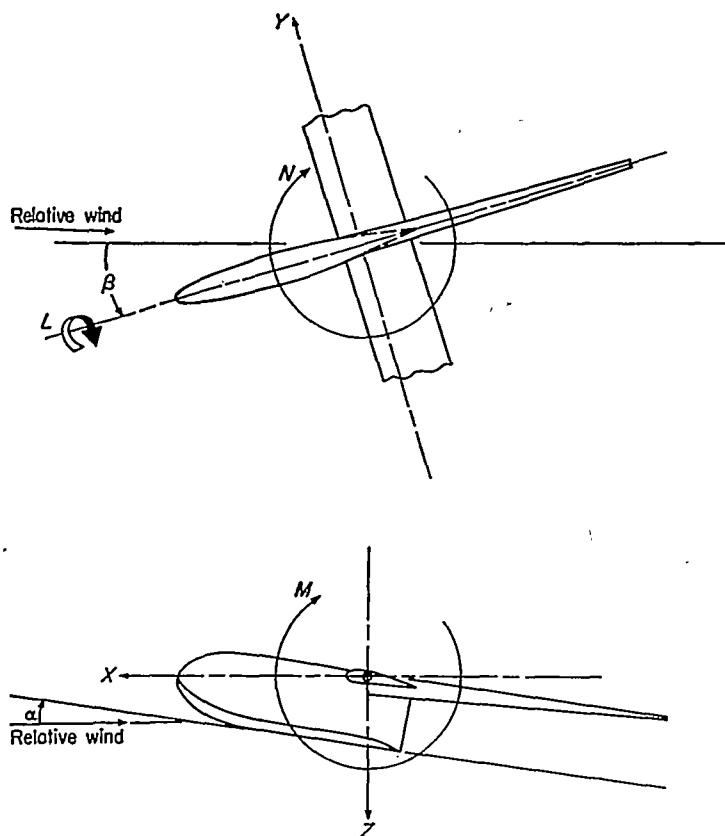


FIGURE 4.—System of stability axes. Positive values of forces, moments, and angles are indicated by arrows.

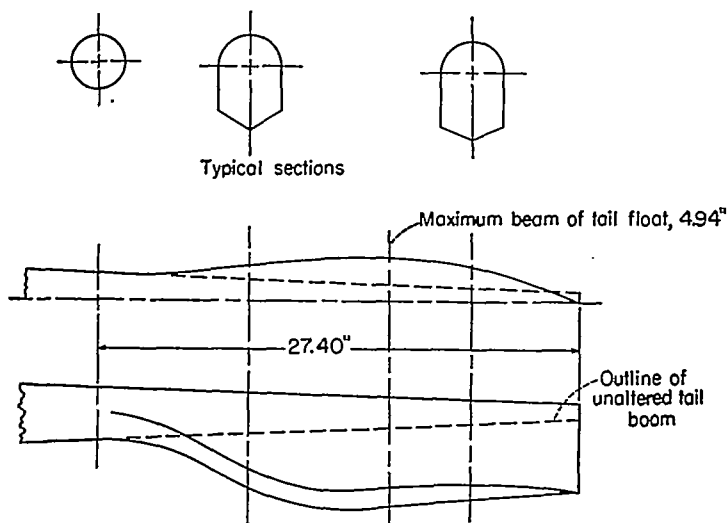


FIGURE 5.—Lines of tail float incorporated on hulls 237-5F1 and 237-7F1.

about 9, represents the fuselage of a typical high-speed land-plane; dimensions are given in figure 3 and table VI. The engine nacelle (fig. 6) was a scale model of the engine nacelle of the XPBB-1 flying boat (ref. 1). The manner in which the engine-nacelle boom was derived is also shown in figure 6. Photographs of the hulls with the corresponding Langley

tank designation numbers are given in figure 7. All models and interchangeable parts were constructed of laminated mahogany and finished with pigmented varnish. The volumes, surface areas, maximum cross-sectional areas, and side areas for the hulls and fuselage are given in table VII.

The hull was attached to a wing which was mounted horizontally in the tunnel as shown in figure 8. The wing was the one used in the investigations of reference 1. It was set at an incidence of 4° with respect to the base line on all models and had a 20-inch chord, a 94.2-inch span, and an NACA 4321 airfoil section.

TESTS

TEST CONDITIONS

The tests were made in the Langley 300 MPH 7-by 10-foot tunnel at dynamic pressures of approximately 25, 100, and 170 pounds per square foot, corresponding to airspeeds of 100, 201, and 274 miles per hour. Reynolds numbers for these airspeeds, based on the mean aerodynamic chord of the hypothetical flying boat, were approximately 1.30×10^6 , 2.50×10^6 , and 3.10×10^6 , respectively. Corresponding Mach numbers were 0.13, 0.26, and 0.35.

CORRECTIONS

Blocking corrections have been applied to the wing and wing-plus-hull data. The drag coefficients of the hulls and fuselage have been corrected for longitudinal buoyancy effects caused by a tunnel static-pressure gradient. Angles of attack have been corrected for structural deflections caused by aerodynamic forces.

TEST PROCEDURE

The aerodynamic characteristics of the hulls with interference of the support wing were determined by testing the wing alone and the wing-and-hull combinations under identical conditions. The hull aerodynamic coefficients

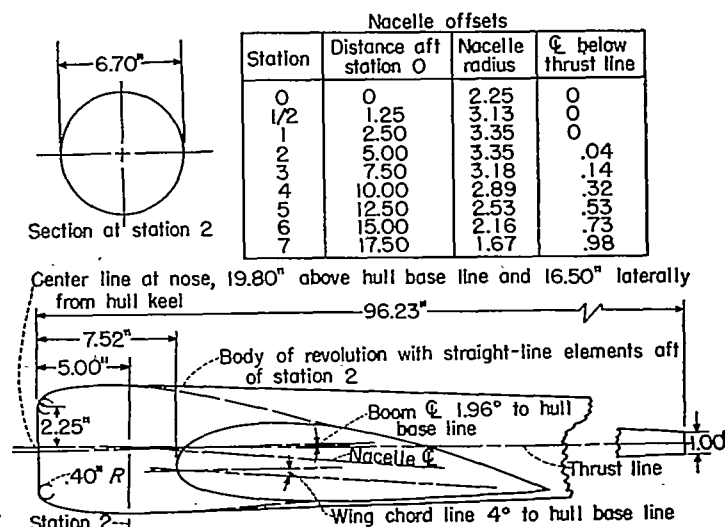


FIGURE 6.—Lines of engine nacelle and engine-nacelle boom.

were determined by subtraction of wing-alone coefficients from wing and hull coefficients after the data were plotted in order to account for structural deflections.

Tests were made at three Reynolds numbers. Because of structural limitations of the support wing, it was necessary to limit the data at the higher Reynolds numbers to the angle-of-attack range shown.

In order to minimize possible errors resulting from transition shift on the wing, the wing transition was fixed at the leading edge by means of roughness strips of carborundum particles of approximately 0.008-inch diameter. The particles were applied for a length of 8 percent airfoil chord measured along the airfoil contour from the leading edge on both upper and lower surfaces.

Hull transition for all tests was fixed by a $\frac{1}{2}$ -inch strip of 0.008-inch-diameter carborundum particles located approximately 5 percent of the hull length aft of the bow. All tests were made with the support setup shown in figure 8.

RESULTS AND DISCUSSION

The aerodynamic characteristics in pitch of the refined deep-step planing-tail hulls with various afterbody configurations are presented in figures 9 and 10 and the aerodynamic characteristics in sideslip, in figures 11 and 12. The aerodynamic characteristics of the streamline fuselage are included in figures 9 and 11. The aerodynamic characteristics in pitch of models incorporating the engine nacelle and the engine-nacelle boom are presented in figures 13 and 14 and the aerodynamic characteristics in sideslip, in figures 11 and 12. The aerodynamic characteristics of the engine nacelle and the engine-nacelle boom without the hull are included in figure 13 (a); the coefficients are plotted against hull angle of attack and therefore correspond to the increments that result from the nacelle or the nacelle boom when the hull is at a given attitude. Minimum drag coefficients and stability parameters, as determined from the figures, are presented in table VIII for comparison.

The following discussion of the longitudinal characteristics is based on the results for Reynolds number 2.5×10^6 . A comparison of figures 9 and 10 indicates that for corresponding configurations the hull models incorporating a forebody with a length-beam ratio of 7 had lower minimum drag coefficients than the hull models incorporating a forebody with a length-beam ratio of 5. The incremental difference in minimum drag coefficient between corresponding configurations varied from 0.0008 for the hull forebodies alone ($C_{D_{min}} = 0.0032$ for model 237-5 and 0.0024 for model 237-7) to 0.0003 for the deep-center-boom configuration ($C_{D_{min}} = 0.0030$ for model 237-5P and 0.0027 for model 237-7P).

According to reference 5, the difference in minimum profile-drag coefficients between airfoil sections of thickness ratios 0.20 and 0.143 is about 20 percent; the difference in

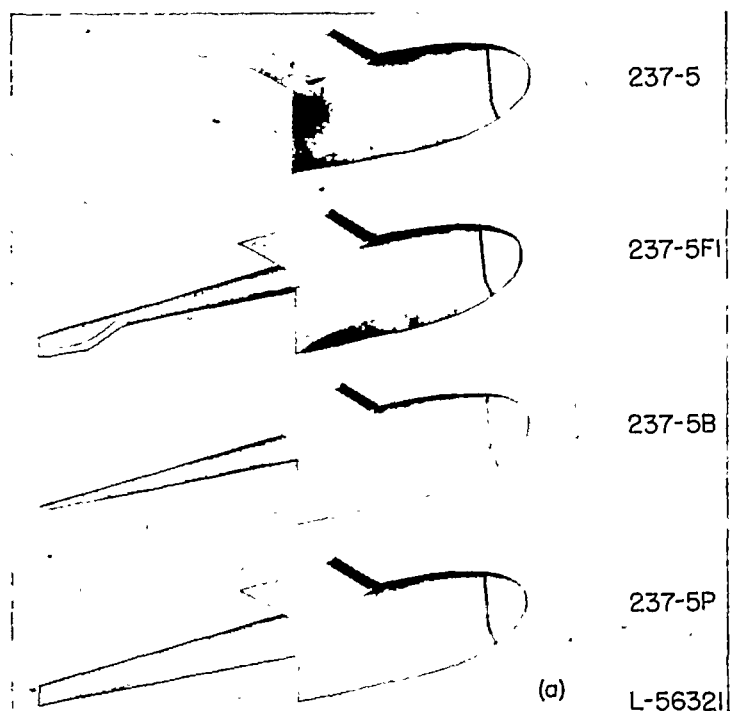


FIGURE 7.—Hull models tested in the Langley 300 MPH 7-by-10-foot tunnel.

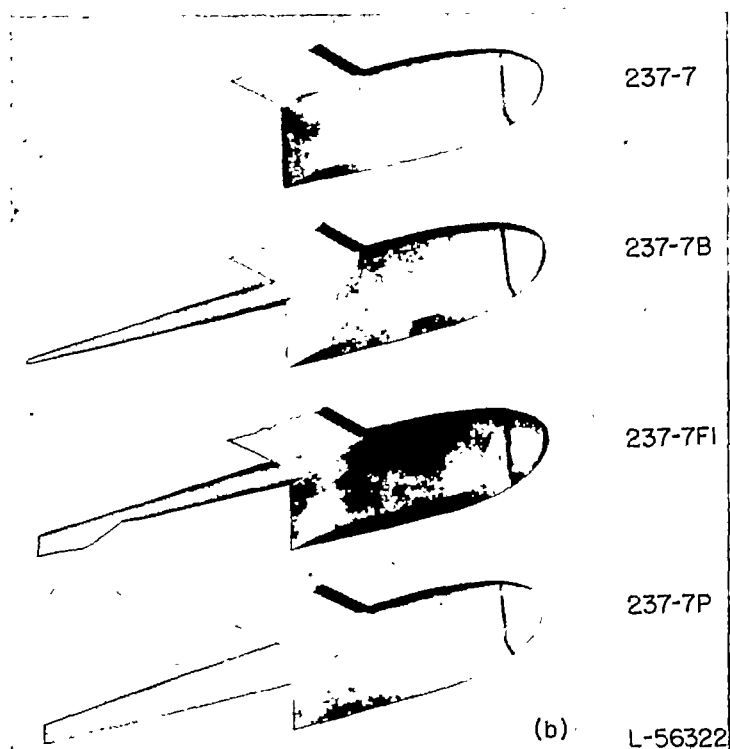


FIGURE 7.—Continued.

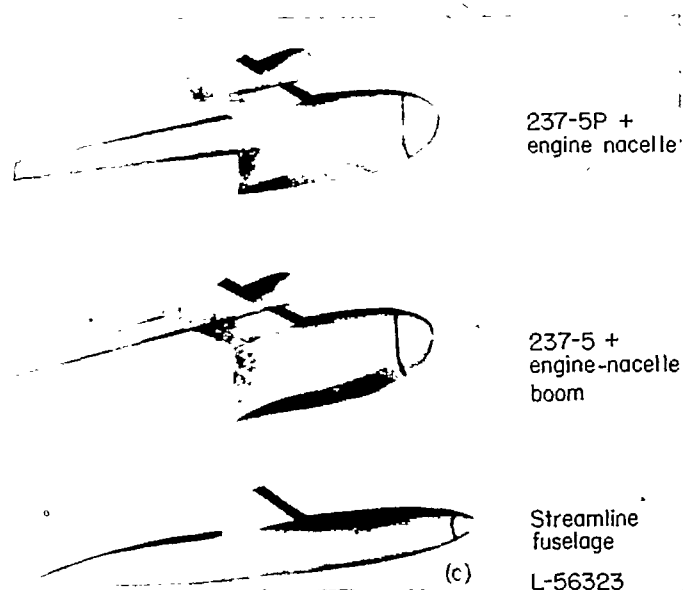


FIGURE 7.—Concluded.

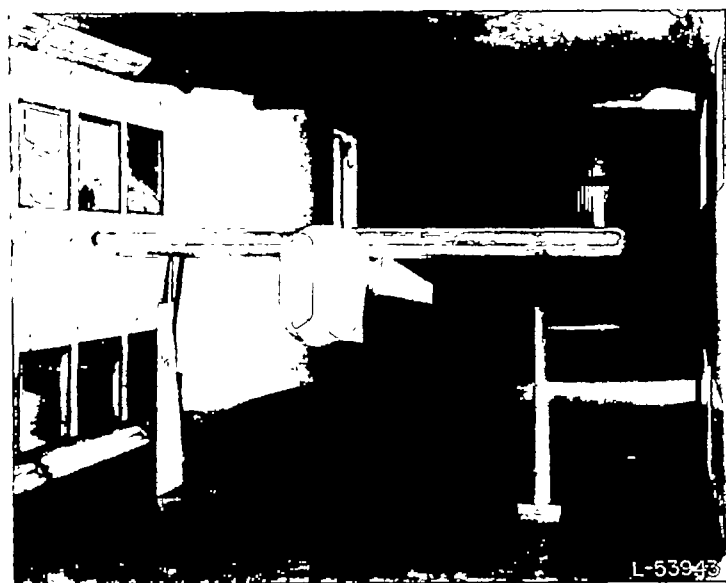


FIGURE 8.—Langley tank model 237-5P mounted in the Langley 300 MPH 7-by 10-foot tunnel.

minimum drag coefficients between hull models 237-7 and 237-5 which were derived from airfoils of these same corresponding thickness ratios agreed favorably with this value.

At negative angles of attack the drag coefficients for hulls with forebody length-beam ratios of 5 were much larger than those for hulls with length-beam ratios of 7 (figs. 9 and 10). The steep drag rise at negative angles can be explained by an examination of the tuft studies of hull models 237-5B, 237-5, 237-7B, and 237-7 presented in figures 15, 16, 17, and 18, respectively. For the length-beam-ratio-5 forebody

alone (fig. 16) a large amount of separation occurred on the upper rear of the forebody and rear of the wing. Fairing the juncture with the boom (fig. 15) reduced the separation somewhat and consequently the hull drag coefficient. Little or no separation occurred for the length-beam-ratio-7 forebody configurations throughout the angle-of-attack range tested (figs. 17 and 18). Unpublished tests of the hulls alone have indicated that the separation was caused primarily by the interference effect of the support wing; tuft studies of the hulls alone at angles of attack corresponding to those of the present report showed no occurrence of separation.

The lowest minimum drag coefficients, 0.0024 and 0.0023, were obtained on hull models 237-7 and 237-7B, respectively. Although the skin area of model 237-7B was larger than that of model 237-7 (table VII) because of the addition of the boom, the drag increase corresponding to the added skin friction was probably offset by the boom's causing a better flow condition at the wing-hull juncture.

As indicated by figures 9 and 10, the hull angle of attack for minimum drag varied from 2° to 4° .

A comparison of the lowest minimum drag coefficient, 0.0023 for hull 237-7B, with that of a conventional hull, 0.0066 for hull model 203 of length-beam ratio 9 (ref. 1), indicated a minimum-drag-coefficient reduction of 0.0043 or 65 percent.

The minimum drag coefficient for the streamline body was 0.0025 (fig. 9); flying-boat hulls can, therefore, have drag values comparable to that of a fuselage of a landplane approximately similar in size and gross weight to a hypothetical flying boat incorporating hull model 237-7B. Tank tests (ref. 4) have shown that a flying boat incorporating hull 237-7B and a gross weight similar to a landplane incorporating the streamline fuselage will take off from and land on water if a small vertical chine strip is added to the hull. There are several disadvantages to this type of hull, however. The hull volume is less than the fuselage volume (table VII) and, because of the location of the major portion of hull volume ahead of the wing where the pay load would be carried, a balance problem would probably be encountered on large flying-boat designs. These disadvantages are much less serious on model 237-7P because of the deep tail boom; the increase in minimum drag coefficient, 0.0004, may be worth the alleviation of the volume and balance problem.

Hydrodynamic considerations have indicated that improved hydrodynamic performance on the deep-step hulls might be facilitated by incorporating a tail float on the hulls such as shown in figure 5. If tank tests indicate that a tail float is much desired, a more refined float than that shown in figure 5 should be used. The minimum drag coefficients of the hull models with tail float, models 237-5F1 and 237-7F1, were 0.0043 and 0.0038, respectively. These

drag-coefficient values were about 0.0015 larger than similar configurations without the tail float.

Figures 9 and 10 show negative values of hull lift coefficient throughout most of the angle-of-attack range tested; the values are especially more negative than those of conventional hulls (ref. 1) in the minimum drag range. In order to compensate for these negative values, the wing lift coefficient of flying boats would have to be increased; this increase would result in an increase in induced-drag coefficient. However, the increase in induced drag for the wing of the hypothetical flying boat, used as a basis in the present investigation, would be small and would not seriously alter the relative merits in performance of the hulls of the present investigation over conventional hulls.

In order to make a preliminary study of overall flying-boat configurations, tests were also made on a typical engine nacelle and an engine nacelle extended into a boom (fig. 6) which is to function as the afterbody and reduce the size of, or possibly eliminate, wing-tip floats. The drag coefficients for one engine nacelle and one engine-nacelle boom near the angle of attack for minimum drag of the hulls without nacelles were about equal, with a value of 0.0022 (fig. 13 (a)). This drag coefficient agreed favorably with the increment of drag coefficient resulting from the addition of the engine nacelle or the engine-nacelle boom to the hull models as determined by a comparison of figures 13 and 14 with figures 9 and 10. The drag coefficient for the nacelle alone and nacelle boom alone decreased as the hull angle of attack became less positive. A more rapid decrease occurred for the nacelle alone; this effect probably accounts for the negative shift in angle of attack for minimum drag of the forebody alone plus the engine nacelle.

The minimum drag coefficients for both combinations were about equal so that a flying-boat configuration with twin engine-nacelle booms probably has an advantage in aerodynamic performance over a flying boat with a single round boom and conventional nacelles resulting from the reduction in size of, or possible elimination of, wing-tip floats. As noted previously, the length-beam-ratio-5 forebody alone had a greater drag than the forebody with a round center boom, mainly because of an adverse wing interference effect. However, the configuration with nacelle booms still might be better aerodynamically, especially if the wing-hull junction had a suitable fairing. These results show the need for investigation of overall flying-boat hull configurations if further progress is to be made in improving the aerodynamic performance of flying boats.

The longitudinal stability for the various hulls, as indicated by the parameter C_{m_α} , is given in table VIII. The hull models incorporating a forebody with a length-beam ratio of 7 were generally less unstable longitudinally than those with a length-beam ratio of 5. This increase in longitudinal stability with length-beam ratio is similar to that reported

in reference 1. As expected, because of the large part of the hull ahead of the center of moments, the most longitudinally unstable hull models were forebody-alone configurations 237-5 and 237-7 which had C_{m_α} values of 0.0028 and 0.0026, respectively. The addition of afterbodies had only a small effect on the stability which corresponds to a rearward aerodynamic-center shift of less than 1 percent mean aerodynamic chord on a flying boat. Of the models tested, the choice of hulls probably should be determined mainly from hull drag, hull volume, and balance considerations; the increase in horizontal-tail area necessary to compensate for the hulls with less stability would give only a small drag increase which would be blanketed by the reduction obtained by using the lower drag hulls. These factors should also be considered when comparison is made with the conventional-type hulls of reference 1. The deep-step hulls were slightly less unstable longitudinally for the present wing and center-of-gravity positions, which were located from hydrodynamic considerations.

The directional stability as determined by C_{n_β} (table VIII) was -0.0008 for hull model 237-5 and -0.0009 for model 237-7. As expected, the addition of the afterbodies reduced the directional instability slightly, the amount depending upon the amount of side area added and its location aft of the center of moments. The least directionally unstable configurations tested were models 237-5P and 237-5F1 which both had a C_{n_β} value of -0.0006. The increase in directional instability with length-beam ratio is also similar to that reported in reference 1 and probably resulted from the increase in side area ahead of the center of moments with length-beam ratio.

The addition of the engine nacelle to models 237-5 and 237-7B increased C_{m_α} slightly but showed no change in C_{n_β} . The directional stability of the flying-boat hulls of the present investigation was generally about the same as that of conventional hulls. This result can largely be explained by the fact that the different center-of-gravity positions compensated for the difference in body shape.

CONCLUSIONS

The results of tests in the Langley 300 MPH 7- by 10-foot tunnel to determine the aerodynamic characteristics of refined deep-step planing-tail flying-boat hulls with various forebody and afterbody shapes and a streamline fuselage indicate the following conclusions:

1. For corresponding configurations the hull models incorporating a forebody with a length-beam ratio of 7 had lower minimum drag coefficients than the hull models incorporating a forebody with a length-beam ratio of 5.

2. The lowest minimum drag coefficients, 0.0024 and 0.0023, which were about 65 percent less than that of a comparable conventional hull of a previous investigation,

were obtained on the length-beam-ratio-7 forebody, alone and with round center boom, respectively.

3. The minimum drag coefficient obtained for the streamline body was 0.0025; flying-boat hulls can, therefore, have drag coefficients comparable to landplane fuselages.

4. The hull angle of attack for minimum drag varied from 2° to about 4° .

5. Longitudinal and lateral stability was generally about the same for all hull models tested and about the same as a conventional hull of a previous aerodynamic investigation.

LANGLEY AERONAUTICAL LABORATORY,
NATIONAL ADVISORY COMMITTEE FOR AERONAUTICS,
LANGLEY FIELD, VA., June 30, 1948.

REFERENCES

1. Yates, Campbell C., and Riebe, John M.: Effect of Length-Beam Ratio on the Aerodynamic Characteristics of Flying-Boat Hulls. NACA TN 1305, 1947.
2. Riebe, John M., and Naeseth, Rodger L.: Aerodynamic Characteristics of Three Deep-Step Planing-Tail Flying-Boat Hulls. NACA RM L8I27, 1948.
3. Suydam, Henry B.: Hydrodynamic Characteristics of a Low-Drag, Planing-Tail Flying-Boat Hull. NACA TN 2481, 1952. (Supersedes NACA RM L7I10.)
4. McKann, Robert, and Coffee, Claude W.: Hydrodynamic Characteristics of Aerodynamically Refined Planing-Tail Hulls. NACA RM L9B04, 1949.
5. Jacobs, Eastman N., Ward, Kenneth E., and Pinkerton, Robert M.: The Characteristics of 78 Related Airfoil Sections From Tests in the Variable-Density Wind Tunnel. NACA Rep. 460, 1933.

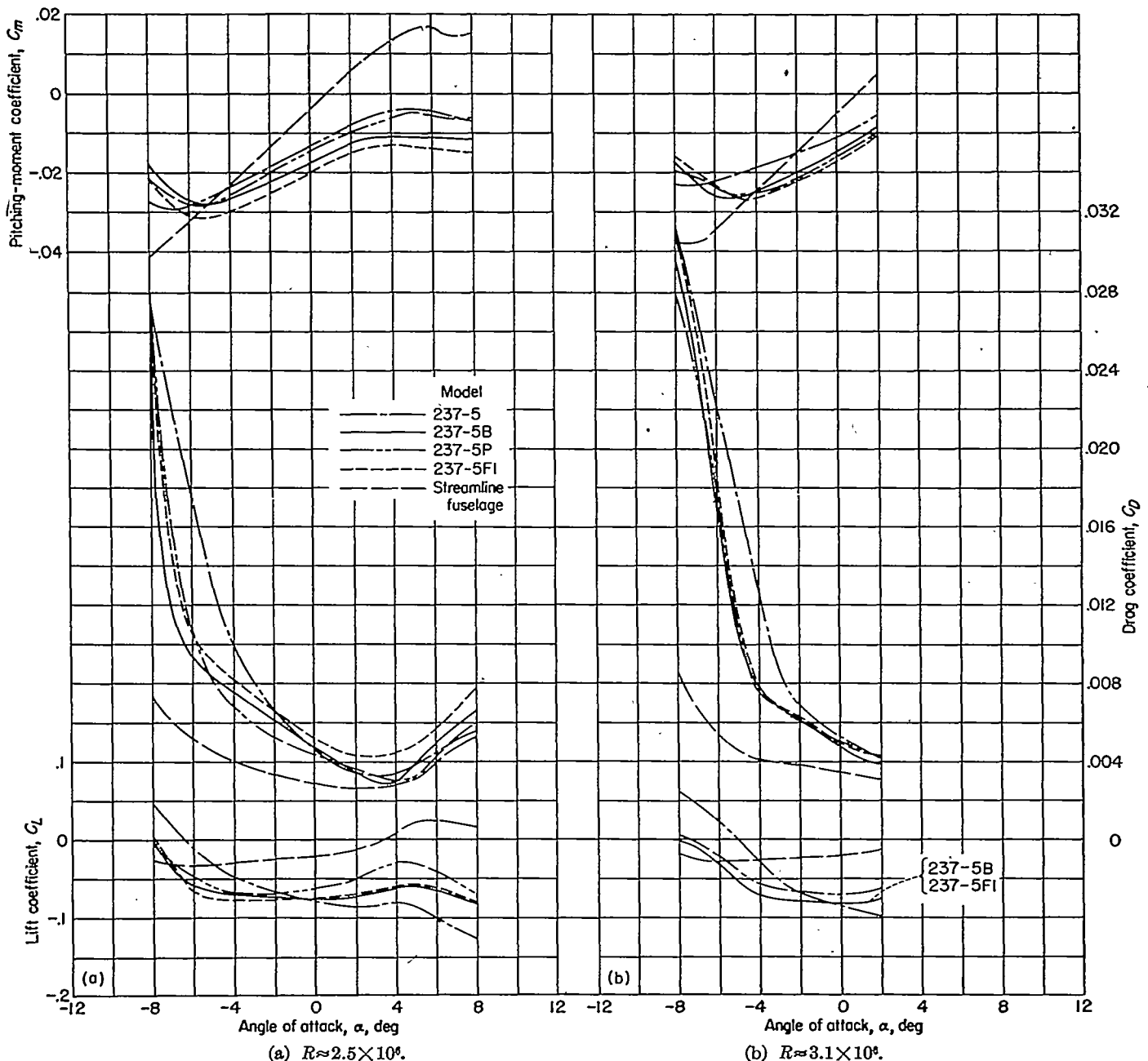


FIGURE 9.—Aerodynamic characteristics in pitch of Langley tank model 237-5 with various afterbody configurations and streamline fuselage.

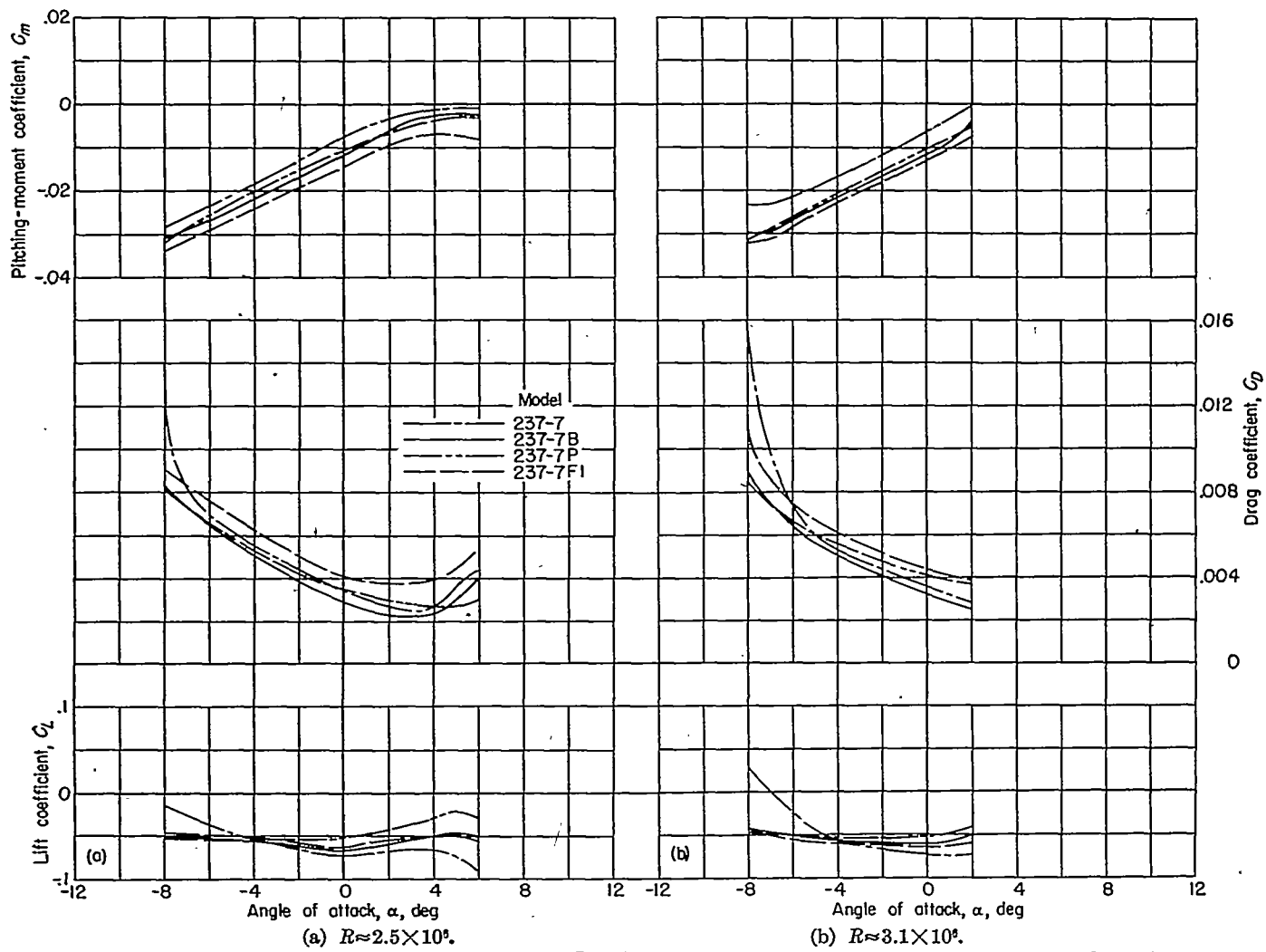


FIGURE 10.—Aerodynamic characteristics in pitch of Langley tank model 237-7 with various afterbody configurations.

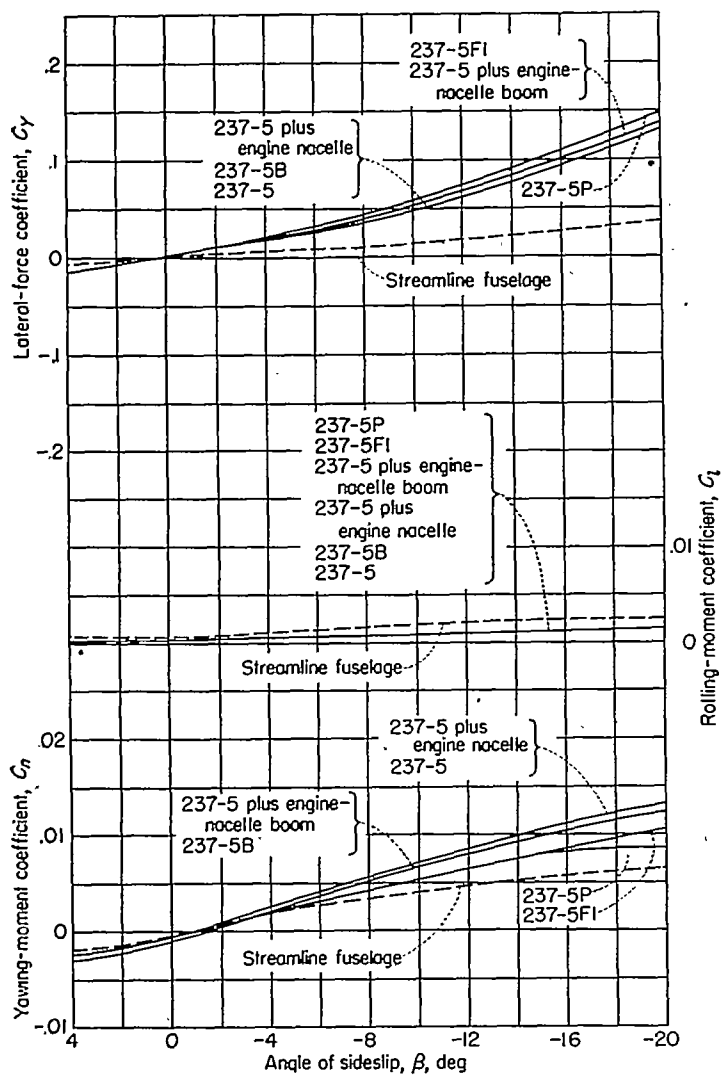


FIGURE 11.—Aerodynamic characteristics in sideslip of Langley tank model 237-5 with various afterbody configurations. $R \approx 1.3 \times 10^6$; $\alpha = 2^\circ$.

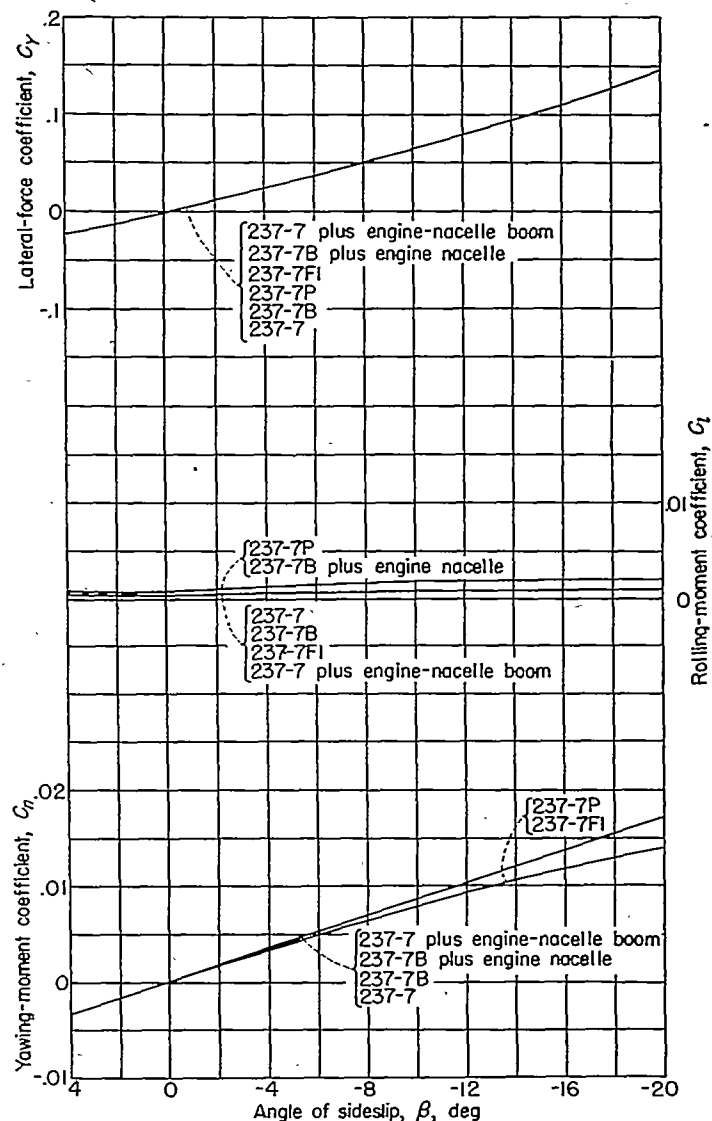


FIGURE 12.—Aerodynamic characteristics in sideslip of Langley tank model 237-7 with various afterbody configurations. $R \approx 1.3 \times 10^6$; $\alpha = 2^\circ$.

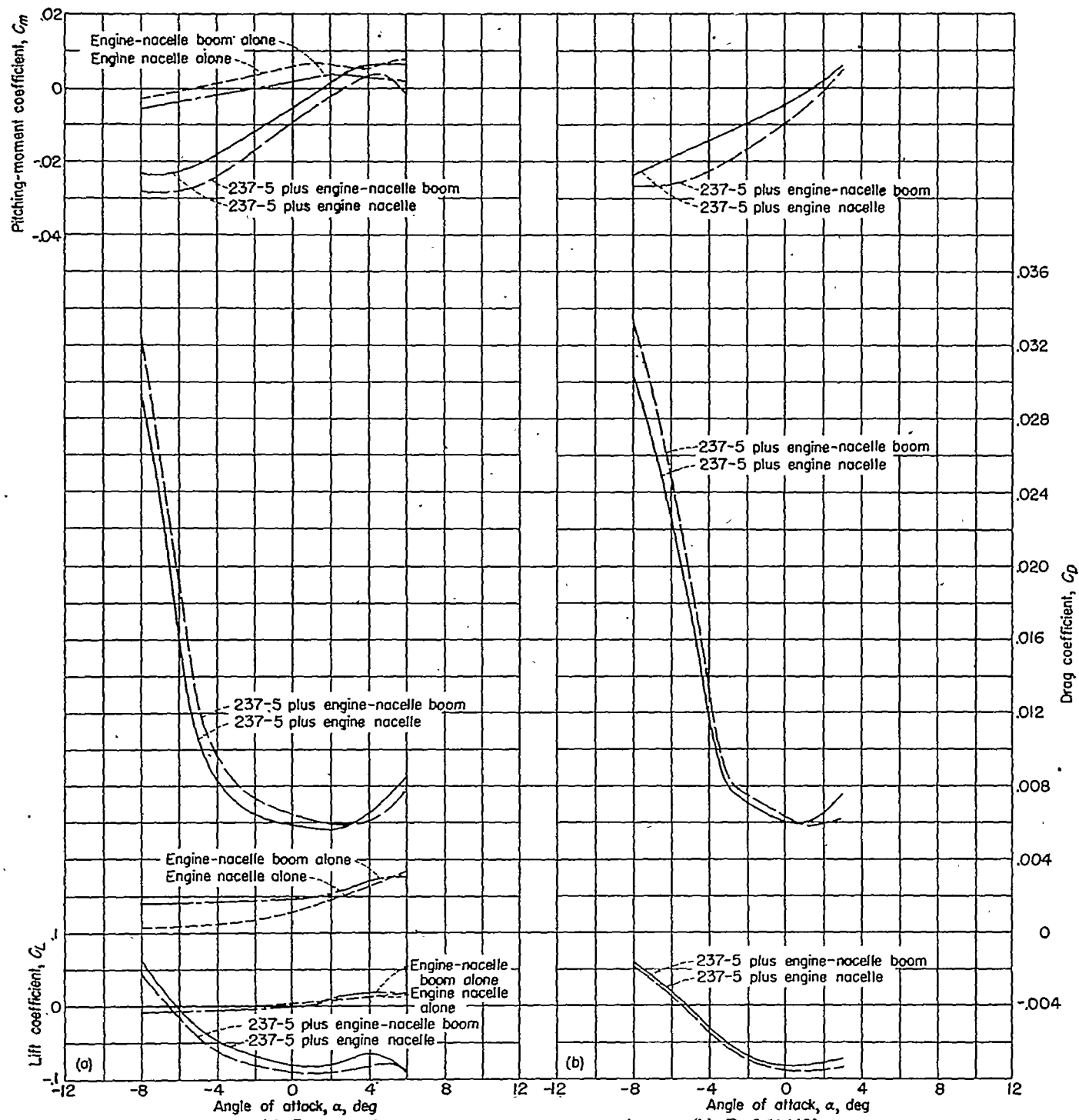


FIGURE 13.—Aerodynamic characteristics in pitch of engine nacelle and engine-nacelle boom alone and with Langley tank model 237-5. The coefficients for the nacelle alone and the nacelle boom alone are given for corresponding hull angles of attack.

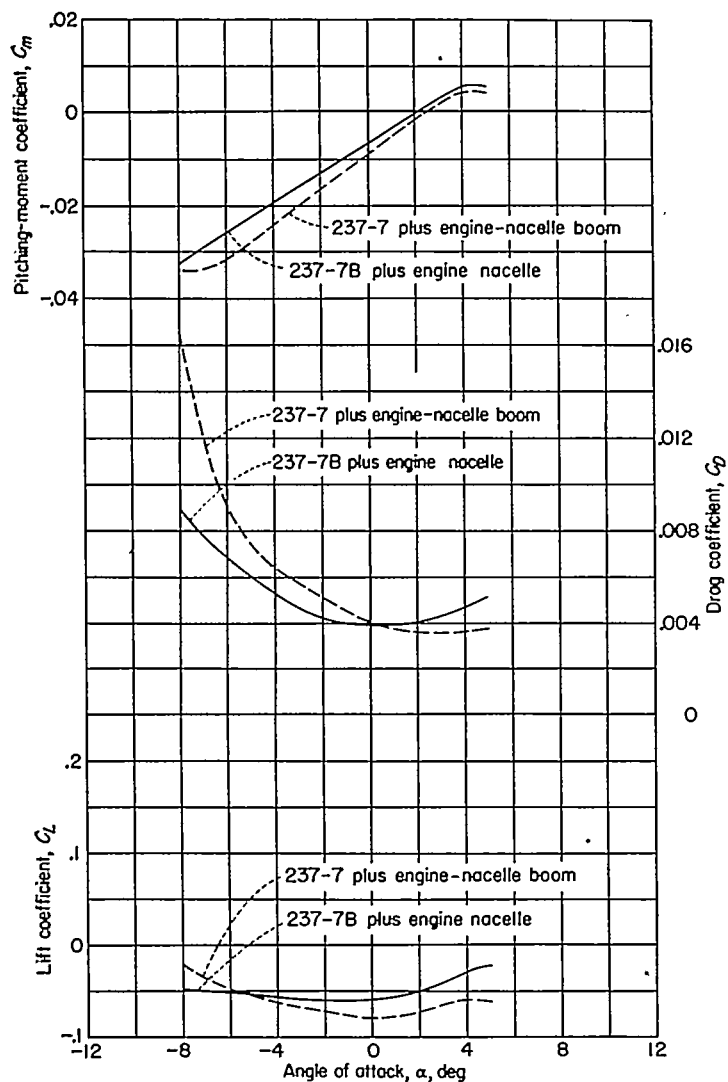
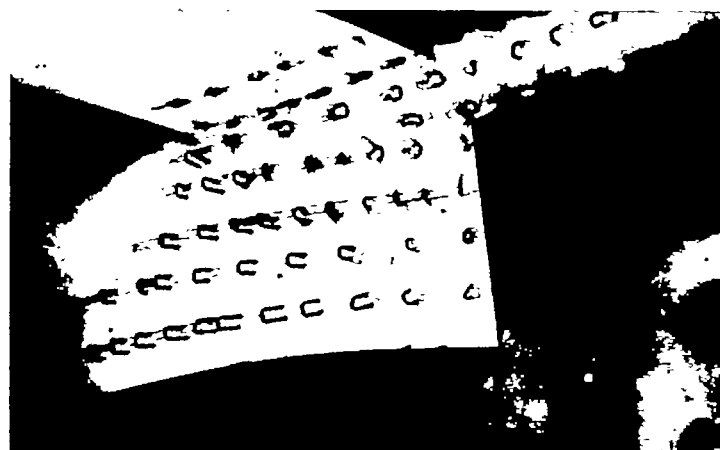
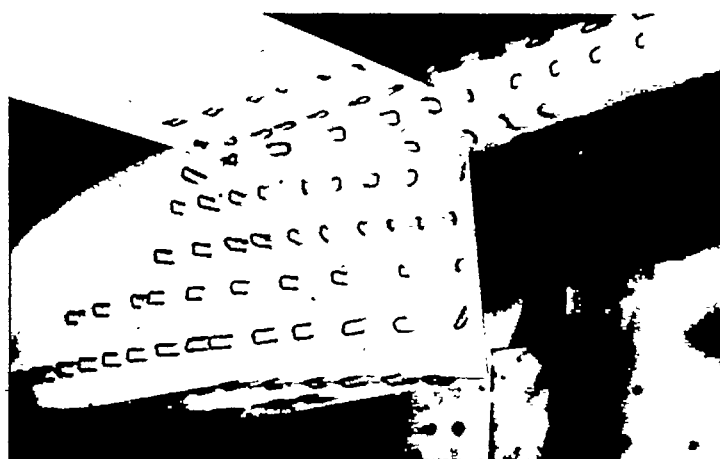


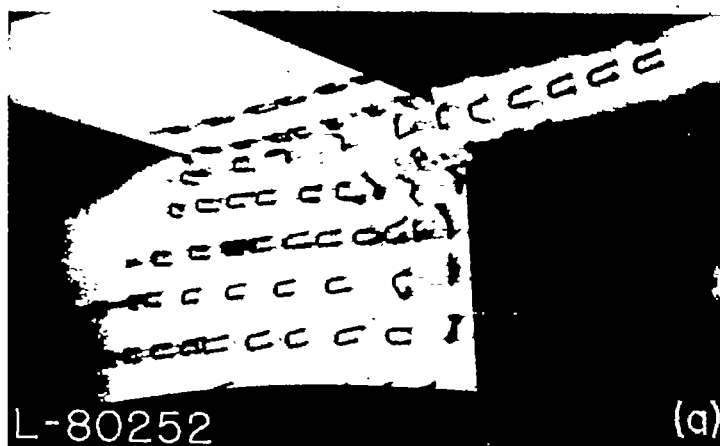
FIGURE 14.—Aerodynamic characteristics in pitch of Langley tank model 237-7 with engine nacelle and engine-nacelle boom, $R \approx 2.5 \times 10^6$.



$\alpha = -8^\circ$



$\alpha = -6^\circ$



$\alpha = -4^\circ$

FIGURE 15.—Tuft studies of Langley tank model 237-5B.

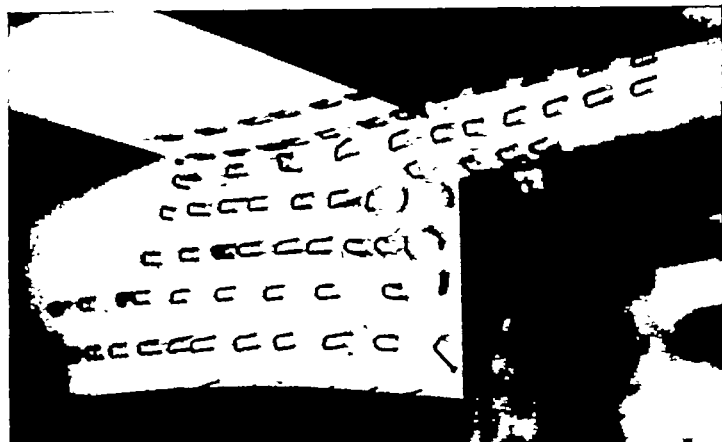
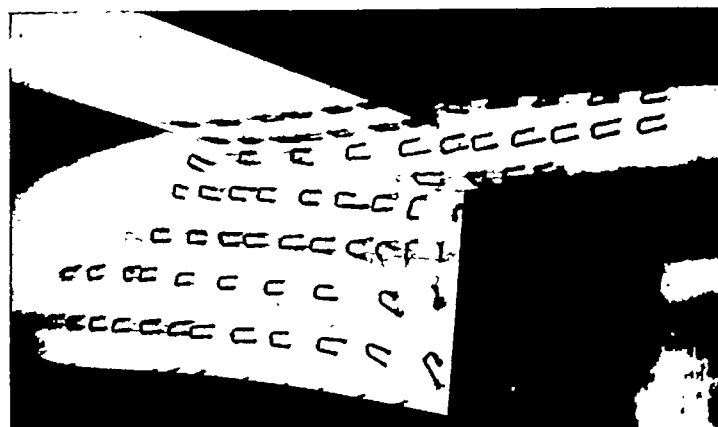
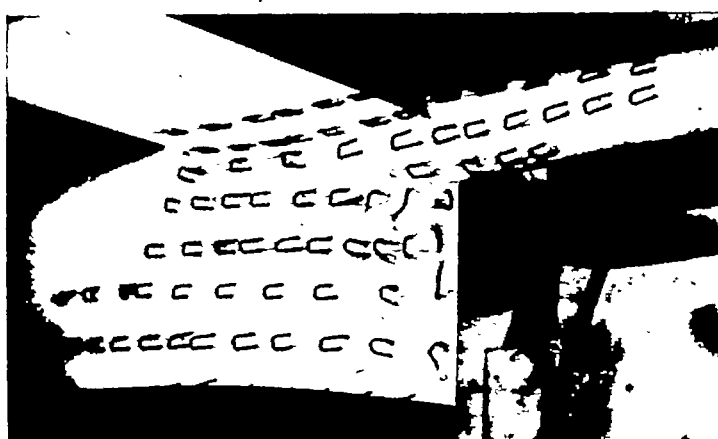
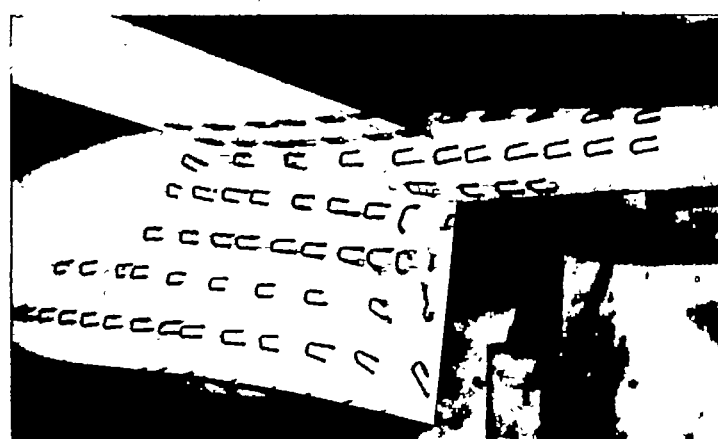
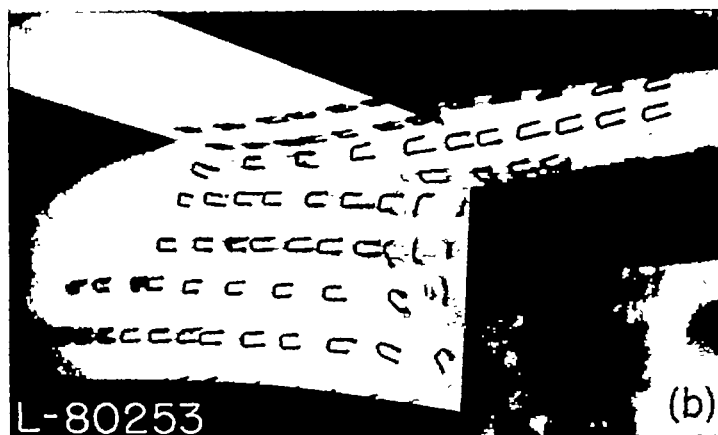
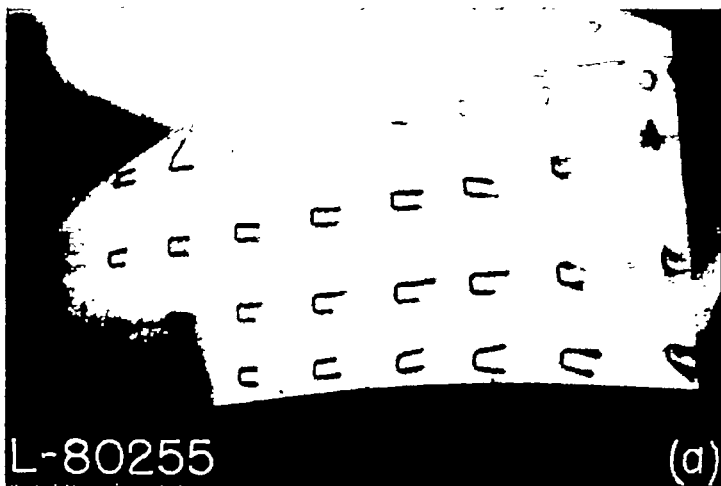

 $\alpha = -2^\circ$

 $\alpha = 4^\circ$

 $\alpha = 0^\circ$

 $\alpha = 6^\circ$

 $\alpha = 2^\circ$

FIGURE 15.—Continued.


 $\alpha = 8^\circ$

FIGURE 15.—Concluded.

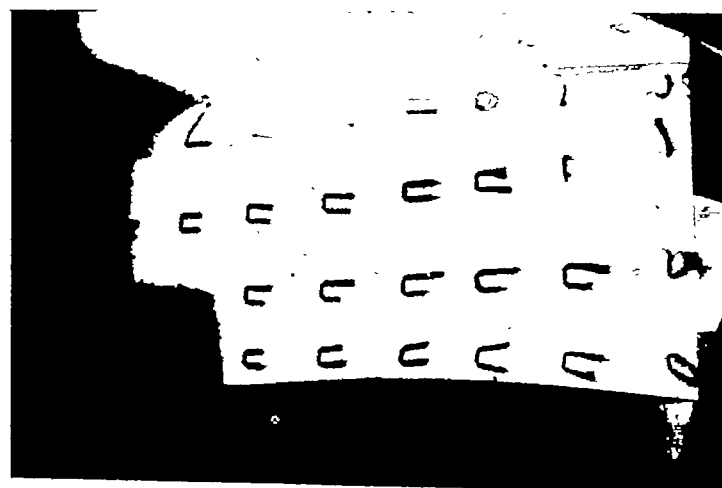
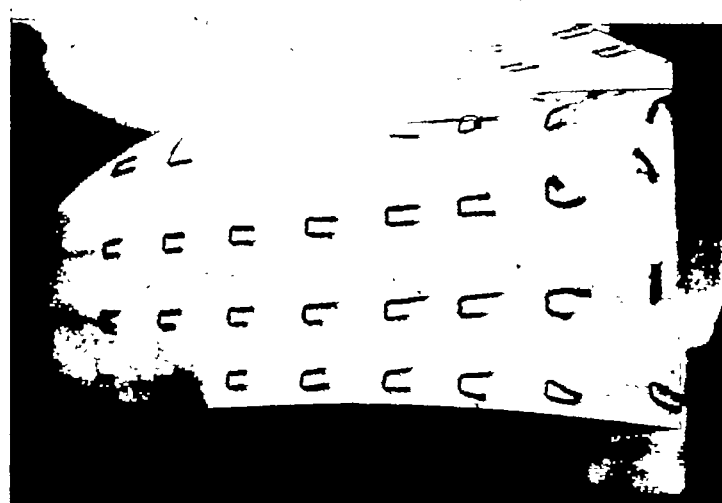

 $\alpha = -8^\circ$

 $\alpha = -6^\circ$

 $\alpha = -4^\circ$

L-80255

(a)

FIGURE 16.—Tuft studies of Langley tank model 237-5.

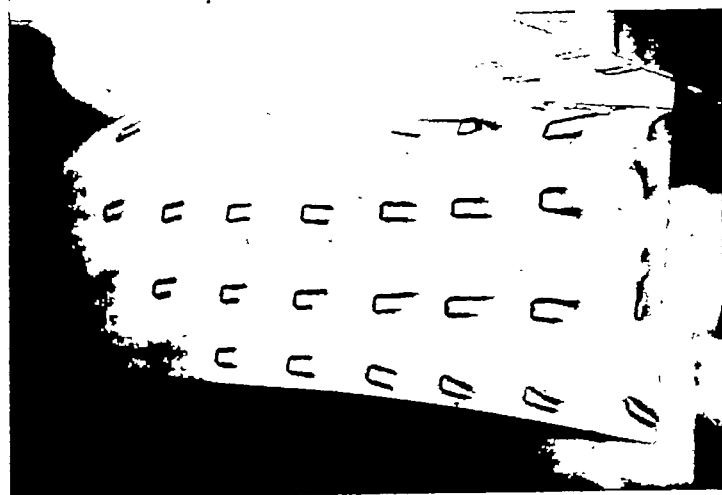
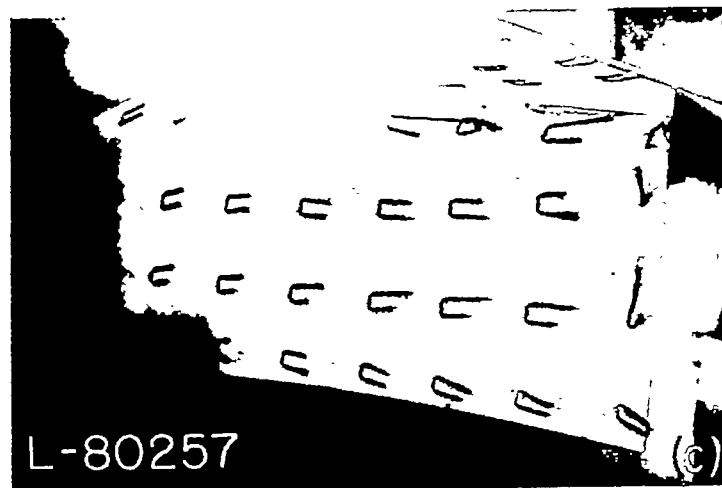

 $\alpha = -2^\circ$

 $\alpha = 0^\circ$

 $\alpha = 2^\circ$

L-80256

(b)

FIGURE 16.—Continued.

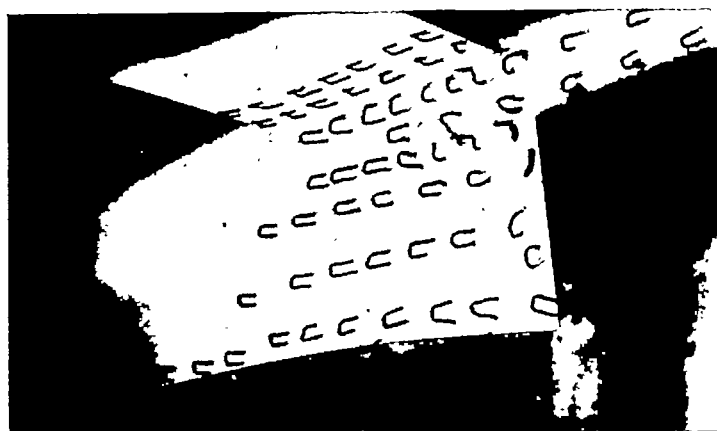
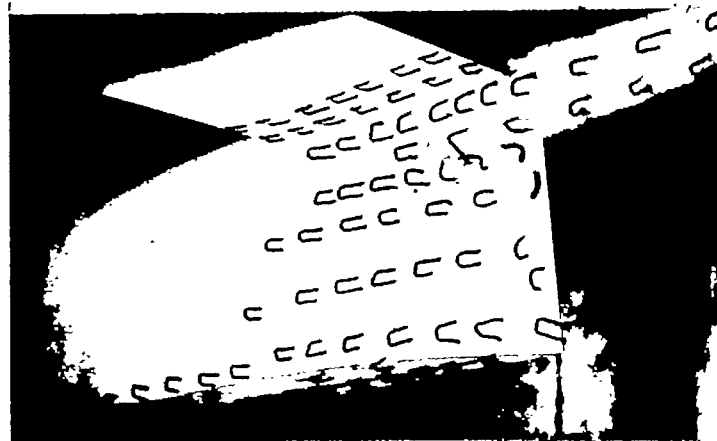
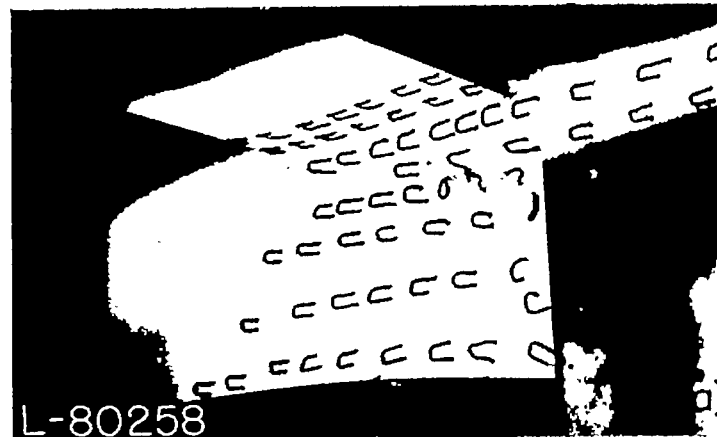

 $\alpha = 4^\circ$

 $\alpha = 6^\circ$


L-80257

(c)

 $\alpha = 8^\circ$

FIGURE 16.—Concluded.


 $\alpha = -8^\circ$

 $\alpha = -6^\circ$


L-80258

(d)

 $\alpha = -4^\circ$

FIGURE 17.—Tuft studies of Langley tank model 237-7B.

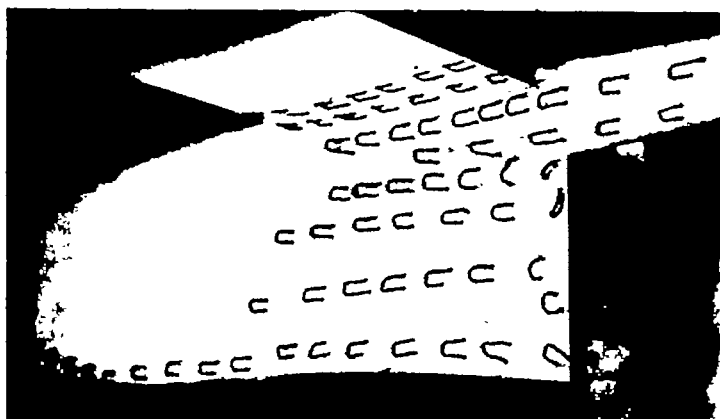
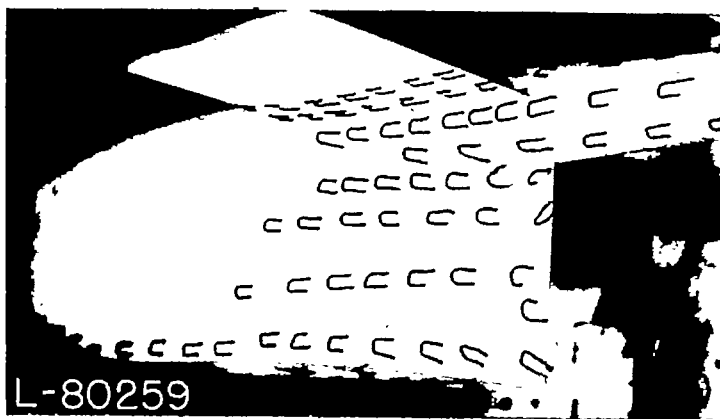
 $\alpha = -2^\circ$  $\alpha = 0^\circ$  $\alpha = 2^\circ$

FIGURE 17.—Continued.

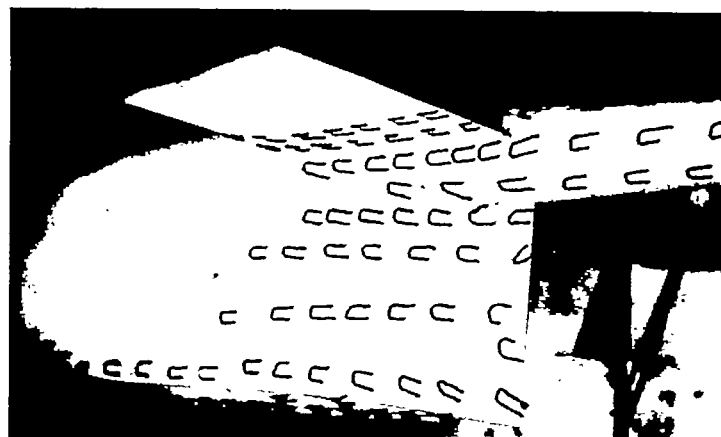
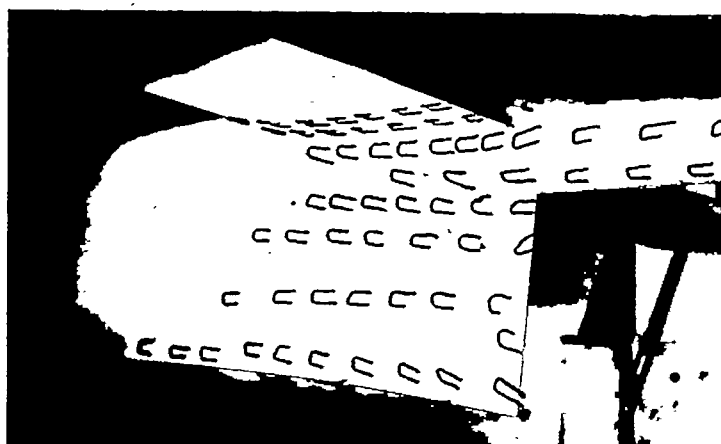
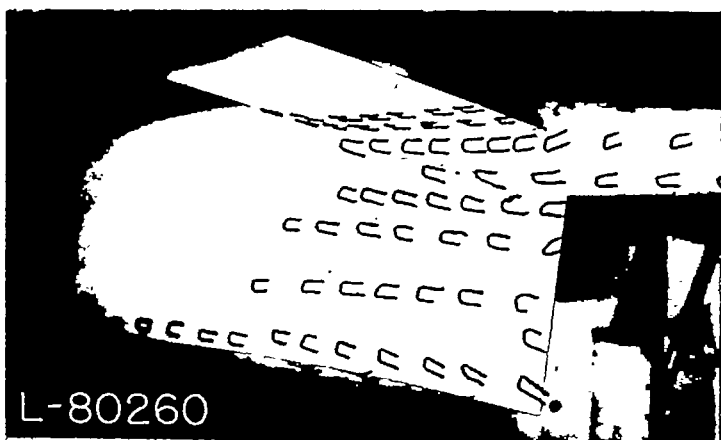
 $\alpha = 4^\circ$  $\alpha = 6^\circ$  $\alpha = 8^\circ$

FIGURE 17.—Concluded.

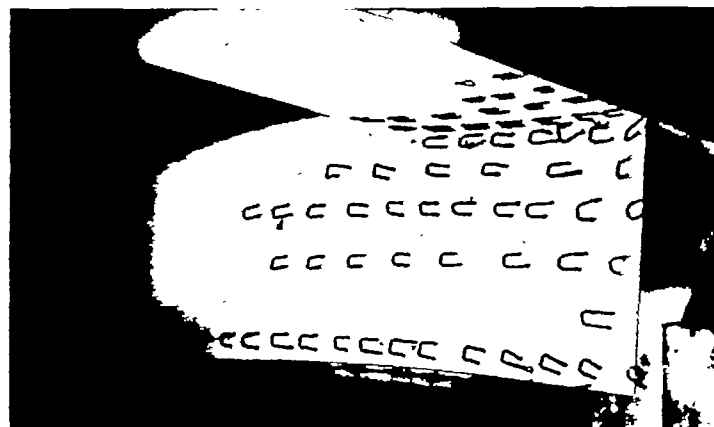
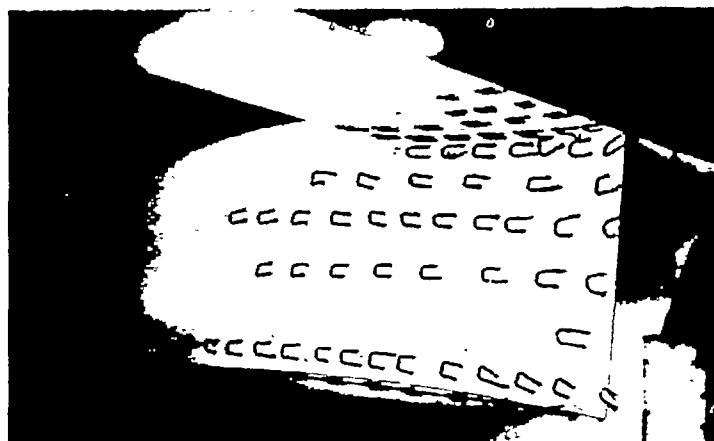
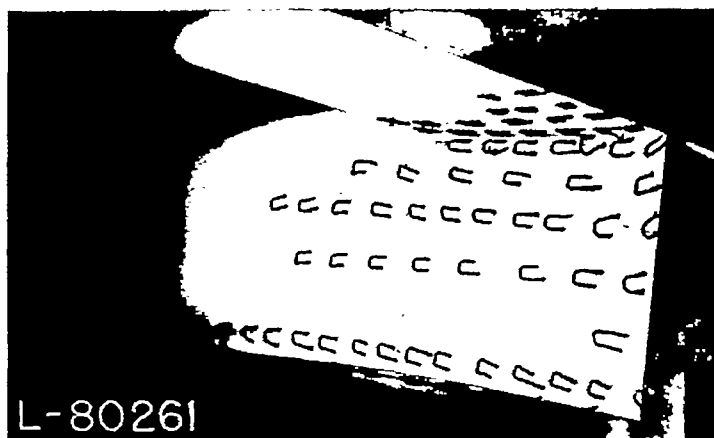
 $\alpha = 4^\circ$  $\alpha = 6^\circ$  $\alpha = 8^\circ$

FIGURE 18.—Tuft studies of Langley tank model 237-7.

TABLE I
OFFSETS FOR LANGLEY TANK MODEL 237-5

[All dimensions are in inches]

[illegible]

TABLE II
OFFSETS FOR LANGLEY TANK MODEL 237-7

[All dimensions are in inches]

[illegible]

TABLE III.
OFFSETS FOR LANGLEY MODELS 237-5B AND 237-7B

Offsets for hull ahead of stations 9 and 7 are given in tables I and II, respectively. All dimensions are in inches.]

Station	Distance to F. P., table I, or distance to station 0, table II	Keel above base line	Chine above base line	Half beam at chine	Radius and half maximum beam	Height of hull at center line	Line of centers above base line
237-5B							
9	38.25	0	1.19	3.28	3.32	19.85	16.53
10	42.50	0	.72	1.98	3.17	19.70	16.53
11	46.75	0	.15	.43	3.00	19.53	16.53
11½	47.90	{ 13.55 }	0	0	2.96	19.49	16.53
237-7B							
7	29.75	0	1.30	3.57	3.62	20.00	16.38
7½	31.87	0	1.25	3.40	3.54	19.97	16.43
8	34.00	0	1.18	3.18	3.46	19.95	16.49
9	38.25	0	.93	2.47	3.32	19.85	16.53
10	42.50	0	.55	1.45	3.17	19.70	16.53
11	46.75	0	.12	.32	3.00	19.53	16.53
11½	47.90	{ 13.55 }	0	0	2.96	19.49	16.53
237-5B and 237-7B							
12	51.00	13.67	-----	-----	2.88	19.39	16.53
13	55.25	13.83	-----	-----	2.70	19.23	16.53
14	59.50	13.98	-----	-----	2.55	19.08	16.53
15	63.75	14.13	-----	-----	2.40	18.93	16.53
16	68.00	14.28	-----	-----	2.25	18.78	16.53
17	72.25	14.44	-----	-----	2.09	18.62	16.53
18	76.50	14.58	-----	-----	1.95	18.48	16.53
19	80.75	14.73	-----	-----	1.80	18.33	16.53
20	85.00	14.90	-----	-----	1.63	18.16	16.53
21	89.25	15.04	-----	-----	1.49	18.02	16.53
22	93.50	15.20	-----	-----	1.33	17.86	16.53
23	97.75	15.36	-----	-----	1.17	17.70	16.53
24	102.00	15.51	-----	-----	1.02	17.55	16.53
25	106.25	15.65	-----	-----	.88	17.41	16.53
26	110.50	15.80	-----	-----	.73	17.26	16.53
27	114.75	15.96	-----	-----	.57	17.10	16.53
A. P.	118.65	16.03	-----	-----	.50	17.03	16.53

TABLE IV
OFFSETS FOR LANGLEY TANK MODELS 237-5P AND 237-7P

[Offsets for hull ahead of stations 9 and 7 are given in tables I and II, respectively. All dimensions are in inches.]

Station	Distance to F. P., table I, or distance to station 0, table II	Keel above base line	Chine above base line	Half beam at chine	Maximum half beam	Height of cove above base line	Height of hull at center line	Line of centers top of hull	Line of centers bottom of hull	1-in. buttock	2-in. buttock	3-in. buttock	10-in. water line	12-in. water line
237-5P														
9	38.25	0	1.19	3.28	3.32	12.37	19.85	16.53	12.82					3.28
10	42.50	0	.72	1.98	3.17	10.33	19.70	16.53	12.80		10.36	11.80		3.05
11	46.75	0	.15	.43	3.00	9.80	19.53	16.53	12.79	9.97	10.55	12.79	1.11	2.89
11½	47.90	9.65	0	0	2.96	9.65	19.49	16.53	12.79	9.99	10.59		1.00	2.85
237-7P														
7	29.75	0	1.30	3.57	3.62	12.24	20.00	16.38	12.84					3.57
7½	31.87	0	1.25	3.40	3.54	11.83	19.97	16.43	12.83					3.45
8	34.00	0	1.18	3.18	3.46	11.43	19.95	16.49	12.83					3.30
9	38.25	0	.93	2.47	3.32	10.62	19.85	16.53	12.82			11.40		3.21
10	42.50	0	.55	1.45	3.17	10.02	19.70	16.53	12.80		10.36	11.80		3.05
11	46.75	0	.12	.32	3.00	9.72	19.53	16.53	12.79	9.97	10.55	12.79	1.11	2.89
11½	47.90	9.65	0	0	2.96	9.65	19.49	16.53	12.79	9.99	10.59		1.00	2.85
237-5P and 237-7P														
13	55.25	9.91	-----	-----	2.70		19.23	16.53	12.77	10.27	10.96		0.25	2.57
15	63.75	10.21	-----	-----	2.40		18.93	16.53	12.75	10.57	11.43			2.27
17	72.25	10.51	-----	-----	2.09		18.62	16.53	12.72	10.91	12.14			1.95
18	76.50	10.67	-----	-----	1.95		18.48	16.53	12.71	11.07				1.82
19	80.75	10.82	-----	-----	1.80		18.33	16.53		11.20				1.70
20	85.00	10.97	-----	-----	1.63		18.16	16.53		11.32				1.60
21	89.25	11.12	-----	-----	1.48		18.01	16.53		11.46				1.48
22	93.50	11.27	11.75	-----	1.33		17.86	16.53		11.63				1.33
24	102.00	11.58	11.95	-----	1.02		17.55	16.53		11.90				1.02
26	110.50	11.88	12.15	-----	0.73		17.26	16.53						1.02
A. P.	118.65	12.10	12.29	-----	0.50		17.03	16.53						.29

TABLE V
OFFSETS FOR TAIL FLOAT INCORPORATED WITH LANGLEY TANK MODELS 237-5F1 AND 237-7F1

[All dimensions are in inches]

Station	Distance to F. P., table I, or distance to station 0, table II	Keel above base line	Chine above base line	Radius of tail boom	Half maximum beam	Height of hull at center line	Line of centers above base line	1/4-in. buttock	1-in. buttock	1 1/2-in. buttock	2-in. buttock	12-in. water line	13-in. water line	14-in. water line	15-in. water line	16-in. water line	18-in. water line
21	89.25	15.05	16.53	1.48	1.48	18.01	16.53	15.14	15.43								
21 1/4	90.31	15.04	16.50	1.44	1.45	17.96	16.51	15.17	15.49								
21 1/2	91.38	14.94	16.35	1.40	1.46	17.93	16.47	15.21	15.54								
21 3/4	92.44	14.70	16.05	1.36	1.50	17.90	16.40	15.14	15.57	16.03							
22	93.50	14.33	15.59		1.56	17.86	16.30	14.73	15.12	15.53							
22 1/4	94.56	13.82	15.04		1.64	17.81	16.17	14.20	14.55	14.93							
22 1/2	95.63	13.28	14.46		1.74	17.78	16.04	13.62	13.95	14.30							
22 3/4	96.69	12.74	13.88		1.86	17.74	15.88	13.04	13.36	13.66							
23	97.75	12.26	13.35		1.98	17.70	15.72	12.54	12.82	13.09							
23 1/4	99.88	11.56	12.56		2.24	17.62	15.38	11.80	12.01	12.24	12.46	0.95					
24	102.00	11.24	12.16		2.41	17.55	15.14	11.43	11.61	11.81	12.60	2.00	1.29				
24 1/4	103.06	11.21	12.10		2.44	17.51	15.07	11.39	11.57	11.76	11.94	2.17	2.41	2.41			
24 1/2	104.13	11.24	12.13		2.47	17.48	15.01	11.41	11.60	11.78	11.96	2.10	2.46	2.44	2.44		
25	106.25	11.38	12.26		2.43	17.41	14.98	11.56	11.74	11.92	12.10	1.70	2.43	2.46	2.46		
26	110.50	11.68	12.39		1.94	17.26	15.32	11.86	12.05	12.23		1.87	1.93	1.93	1.93		
27	114.75	11.98	12.23		.69	17.10	16.41					.04	.69	.69	.69		
A. P.	116.65	12.12	12.12		0	17.03	17.03						0	0	0	0	0.17

TABLE VI
ORDINATES FOR LANDPLANE FUSELAGE

[All dimensions are given in inches]

Station	Radius	Station	Radius
0.158	0.408	50.989	6.440
.527	.838	54.309	6.420
1.054	1.263	58.143	6.354
2.108	1.887	62.267	6.254
3.373	2.462	66.378	6.121
5.059	3.071	69.896	5.980
7.906	3.864	72.557	5.854
8.432	3.989	76.404	5.642
10.804	4.496	79.843	5.420
14.124	5.064	84.033	5.103
17.457	5.492	87.538	4.797
20.580	5.790	91.015	4.451
23.584	6.003	94.494	4.058
26.483	6.156	97.973	3.616
29.513	6.274	101.451	3.118
33.031	6.369	104.837	2.573
36.918	6.436	108.144	1.978
40.185	6.467	111.543	1.293
43.716	6.481	114.521	.624
45.166	6.482	117.050	0
47.524	6.479		

TABLE VII
VOLUMES, SURFACE AREAS, AND MAXIMUM CROSS-SECTIONAL AREAS OF LANGLEY TANK MODELS 237 AND OF STREAMLINE FUSELAGE

Configuration	Volume, cu in.	Surface area, sq in.	Side area, sq in.	Maximum cross-sectional area, sq in.
237-5	5,649	2,095	841	176
237-7	5,228	2,303	964	142
237-5B	6,519	2,884	1,090	176
237-7B	6,174	3,100	1,213	142
237-5F	7,574	3,427	1,359	176
237-7F	7,276	3,645	1,482	142
237-5F1	6,869	3,106	1,177	176
237-7F1	6,524	3,321	1,300	142
Streamline body	10,270	3,630	1,162	132
Engine nacelle	471	406	108	39
Engine-nacelle boom	1,419	1,220	363	39

TABLE VIII
MINIMUM DRAG COEFFICIENTS AND STABILITY PARAMETERS FOR LANGLEY TANK MODELS 237 AND STREAMLINE BODY

[The drag coefficients are given for a Reynolds number of about 2.5×10^6 based on wing M. A. C.]

Model	$C_{D_{min}}$	$C_{m_{\alpha}}$	$C_{n_{\beta}}$	$C_{T_{\beta}}$
237-5	0.0032	0.0028	-0.0008	-0.0042
237-5F	.0030	.0026	-.0006	-.0042
237-5B	.0028	.0025	-.0005	-.0042
237-5F1	.0043	.0026	-.0005	-.0042
237-5 + engine-nacelle boom	.0059	.0037	-.0008	-.0042
237-5 + engine nacelle	.0056	.0034	-.0008	-.0042
237-7	.0024	.0026	-.0009	-.0060
237-7F	.0027	.0024	-.0008	-.0060
237-7B	.0023	.0025	-.0009	-.0060
237-7F1	.0038	.0024	-.0008	-.0060
237-7 + engine-nacelle boom	.0036	.0037	-.0009	-.0060
237-7B + engine nacelle	.0039	.0032	-.0009	-.0060
Streamline body	.0025	.0049	-.0005	-.0015
Engine nacelle	.0021	.0011		
Engine-nacelle boom	.0022	.0009		

* At $\alpha = 3^\circ$ (not minimum drag coefficient).

